

Surface-termination dependent magnetism and strong perpendicular magnetocrystalline anisotropy of a FeRh (001) thin film: A density-functional study

Soyoung Jekal¹, S. H. Rhim^{1,*}, Soon Cheol Hong^{1,†}, Won-joon Son², and Alexander B. Shick³

¹*Department of Physics and Energy Harvest-Storage Research Center,
University of Ulsan, Ulsan, 680-749, Republic of Korea*

²*Samsung Advanced Institute of Technology,
Suwon, 443-803, Republic of Korea*

³*Institute of Physics, ASCR, Na Slovance 2,
CZ-18221 Prague, Czech Republic*

(Dated: September 30, 2018)

Magnetism of FeRh (001) films strongly depends on film thickness and surface terminations. While magnetic ground state of bulk FeRh is G-type antiferromagnetism, the Rh-terminated films exhibit ferromagnetism with strong perpendicular MCA whose energy $+2.1 \text{ meV}/\square$ is two orders of magnitude greater than bulk 3d magnetic metals, where \square is area of two-dimensional unit cell. While Goodenough-Kanamori-Anderson rule on the superexchange interaction is crucial in determining the magnetic ground phases of FeRh bulk and thin films, the magnetic phases are results of interplay and competition between three mechanisms: the superexchange interaction, the Zener-type direct-interaction, and magnetic energy gain.

PACS numbers: 68.37.Ef, 75.70.Tj, 75.70.Rf

FeRh alloys have attracted significantly because of their various intriguing physics phenomena including magneto-caloric effect and huge magnetoresistance[1–4]. Transition between antiferromagnetism (AFM) and ferromagnetism (FM) occurs above room-temperature about 350 K and ultra-fast phase transition of magnetic phases in the FeRh alloys is induced by femto-second laser, which have drawn more attention due to possibility of applications for heat-assisted magnetic recording (HAMR)[5–7].

Furthermore, feasibility of room-temperature memories based on the AFM spintronics has been successfully demonstrated in the FeRh alloys very recently utilizing anisotropic magneto-resistance (AMR) of the bistable AFM states[8–10]. This AFM spintronics has some advantages over that based on FM states[8–16] owing to the absence of stray magnetic field from the zero net magnetization and the insensitivity to the external magnetic fields. Regarding FeRh thin films, several experiments have been reported[17–19]. Instead of the G-type antiferromagnetic (G-AFM) in bulk, some thin films exhibit FM states stabilized at the interface with metal, while the FM states are unstable at interface with oxide[17]. Interestingly, it was reported that an electric field of only a few volts is necessary to drive the AFM-FM transition for the epitaxially grown FeRh films on the ferroelectric BaTiO₃ substrate[18]. Also, it was revealed that the spin orientation of the FeRh film on the MgO (001) depends on the strength of lattice strain and magnetic state[19].

In this paper, magnetism and magnetocrystalline anisotropy (MCA) of FeRh films are investigated using first-principles calculations. It is found that magnetism and MCA are significantly affected not only by film thickness but also by the surface-terminations. The Rh-terminated films are more stable in FM state by quite big energy differences relative to the magnetic ground G-AFM state in bulk. Furthermore, the Rh-termination exhibits strong perpendicular MCA of

$+2.1 \text{ meV}/\square$, where \square is two-dimensional (2D) unit cell area. The Fe-terminations, on the other hand, are in G-AFM states as in bulk. The strikingly different behavior of these two terminations is explained mainly in the framework of Goodenough-Kanamori-Anderson (GKA) rule on the superexchange interaction[20, 21] with the Zener-type direct exchange interaction[22] also taken into account.

Density functional calculations are performed using Vienna *ab initio* Simulation package (VASP)[23]. Results by VASP, particularly MCA, have been double-checked with the highly precise full-potential linearized augmented plane wave (FLAPW) method[24]. Generalized gradient approximation (GGA) within projector augmented-wave (PAW) scheme[25] is employed for the exchange-correlation interaction. k meshes of $24 \times 24 \times 24$ and $24 \times 24 \times 1$ in Monkhorst-Pack scheme are used for bulk and films, respectively. For wave function expansions, 500 eV is used for cutoff energy. Convergence with respect to cutoff energy and number of k points are seriously checked. Magnetic structures of the bulk FeRh are illustrated schematically in Fig. 1(a)-(c) for A-, C- and G-type AFM, respectively, where arrows represent the direction of magnetic moments of Fe atoms. To account for the AFM structures, a tetragonal magnetic unit cell, $c(2 \times 2)$ in the xy plane and doubled along the z axis, is taken. To investigate thickness and surface-termination dependent magnetism of the FeRh (001) films, two terminations, Fe- and Rh-termination with thickness from 3- to 15-ML have been taken into account, where we allow relaxation along the z -axis while fixing two-dimensional (2D) lattice constant as the calculated bulk value (3.007 \AA) of the G-AFM.

First, magnetism of bulk FeRh is presented. AFM in G-type is found to be most stable from total energy calculations by 48.3, 56.7, and 187 meV/Fe with respect to FM and AFM in A- and C-type, respectively. Since the C-AFM has the highest energy, it will be excluded in forthcoming discussion if

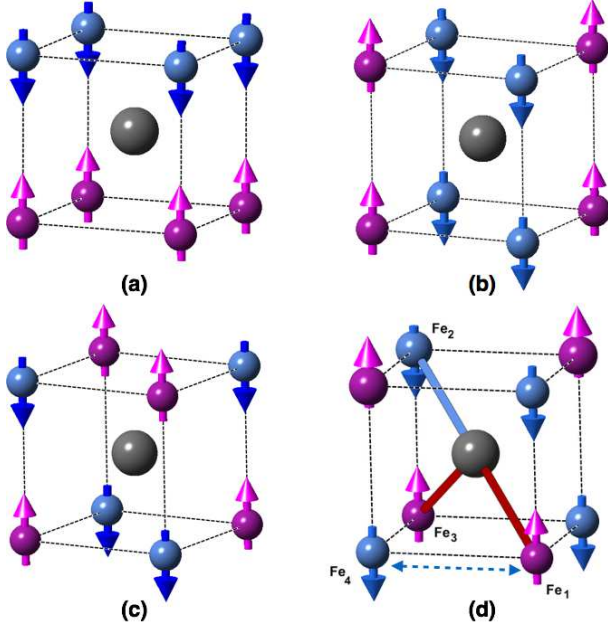


FIG. 1: Schematic diagrams of magnetic structures of (a) A-, (b) C- and (c) G-AFM states of the bulk FeRh, and (d) exchange interaction between Fe atoms in the G-AFM state. Red and blue spheres at the corners represent Fe atoms with different magnetic states, respectively, while grey spheres represent Rh atom. In (d), cylinder connecting Fe_1 and Fe_2 denote the 180° superexchange, while red cylinders connecting Fe_1 -Rh- Fe_3 do the 90° superexchange. Blue dotted line which connects Fe_1 - Fe_4 denotes the direct exchange interaction.

not necessary. Calculated lattice constant (3.012 \AA) of the bulk FeRh in FM state is a little bit larger than that in the G-AFM (3.007 \AA). Magnetic moments of Fe and Rh atoms in the G-AFM (FM) are 3.158 (3.144) μ_B and 0.00 (1.041) μ_B , respectively. Lattice constants and magnetic moments in this work are reasonably consistent with experiments[26, 27] and previous calculation[28].

In FeRh (001) films, the interlayer spacing exhibits oscillatory feature: the topmost surface moves downward whereas the subsurface layers do upward, and so on, where the innermost layer converge to bulk behavior [See Supplementary Information for fully relaxed interlayer spacings of the Fe- and the Rh-terminated film in Fig. S1(a) and (b), respectively]. 7- or 9-ML films are thick enough due to short metallic screening length.

Total energy differences of the FM (A-AFM) and the G-AFM, which we denote as $\Delta E = E_{FM}(E_A) - E_G$, are presented in Fig. 2(a) and (b) for the Fe- and Rh-termination, respectively, where FM, A, and G in subscripts stand for FM, A-AFM, and G-AFM, respectively. As shown in Fig. 2(a), the G-AFM is the most stable for the Fe-termination regardless of thickness. We recall here that magnetism is so delicate physics phenomenon that it can behave differently in reduced dimension[29, 30]. As film gets thinner, ΔE decreases while $\Delta E=36.6 \text{ meV/Fe}$ for 9-ML is still less than that of bulk

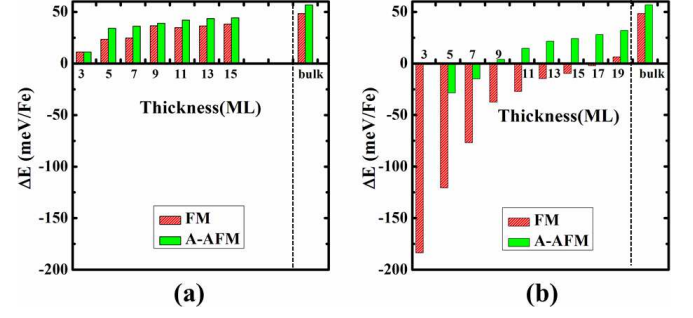


FIG. 2: The thickness dependent total energy differences of the FM and A-AFM states from that of the G-AFM state, $\Delta E = E_{FM}(E_A) - E_G$; (a) the Fe-terminated and (b) the Rh-terminated films.

(48.3 meV/Fe). As shown in Fig. 2(b), magnetism of the Rh-termination is totally different from the bulk. FM is favored over G-AFM up to 15-ML by big energy difference whose absolute value is larger than 70 meV/Fe for 7-ML. Noteworthy, there is a crossover from FM to G-AFM when the number of layers exceeds 17-ML. Furthermore, even A-AFM is more stable than G-AFM for films thinner than 7-ML. Magnetic moments of Fe and Rh atoms in both terminations are listed in Table 1 and 2 for their respective magnetic ground states, G-AFM and FM. The surface layers have almost the same magnetic moments as the bulk unlike other surfaces of magnetic elements, Fe, Co, and Ni, where moments are strongly enhanced.

Before we discuss magnetism the FeRh films, we provide here a detailed analysis of bulk magnetism. e_g and t_{2g} are degenerate in G-AFM and FM due to the cubic symmetry, whereas those in A- and C-AFM are no longer degenerate owing to the tetragonal magnetic structure (see SI Fig. S2). Strong hybridization between Fe and Rh d states brings in almost fully occupied (unoccupied) majority (minority) spin states of Fe d orbital, particularly e_g states for all magnetic phases, which results in enhanced moments of Fe atoms. The nearly half-filled band favors AFM as in bulk Mn and Cr. It is noteworthy that the majority spin bands of Rh are almost fully occupied in the FM similarly to Fe, but featureless in AFM states.

The magnetic phase of FeRh alloy can be explained by interplay between three mechanisms - superexchange interaction[20, 21], Zener-type direct-exchange interaction[22], and magnetic energy gain. In the framework of GKA rule, whether FM or AFM is preferred by superexchange interaction is explained by magnetic ion-ligand-magnetic ion angle. Here we view Fe atoms as magnetic ions and delocalized s and p orbitals of Rh as ligand orbitals in GKA rule. Fig. 1(d) schematically illustrates magnetic interactions between Fe atoms to be involved in determining magnetic structure. The GKA superexchange interactions are shown as solid lines and Zener-type direct interaction as a dotted line. In accord with GKA rule on magnetic coupling, Fe_1 prefers AFM coupling to Fe_2 and FM coupling to Fe_3 because angles of Fe_1 -Rh- Fe_2 and

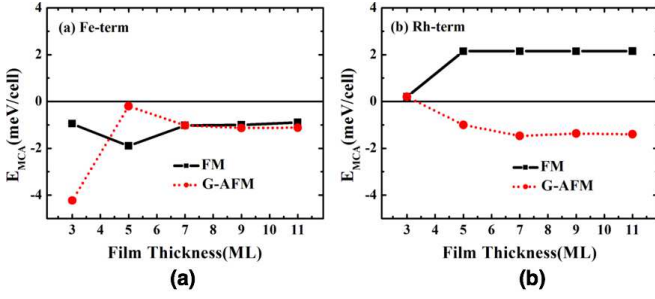


FIG. 3: MCA energies, defined as $E_{MCA} \equiv E(\rightarrow) - E(\uparrow)$, of the FeRh (001) thin films for (a) Fe- and (b) Rh-terminated films, respectively. Solid (dashed) lines denote MCA of FM (G-AFM) phase.

Fe₁-Rh-Fe₃ are 180° and 109.5° (which is close to 90°), respectively.

On the other hand, the interaction between Fe₁ and Fe₄ is more or less direct since Rh atom is not much involved in this coupling. The half-filled e_g states directing along the principal axes are more involved in the Zener direct interaction between Fe₁ and Fe₄ compared to the t_{2g} states, which results in AFM coupling[22]. Since the d states are highly localized giving little wave function overlap, the Zener-type direct interaction between Fe₁ and Fe₄ must be weak. As a result of combination of the superexchange and the direct interactions discussed above, G-AFM is most stable among other AFM states. In the FM states, on the other hand, there is magnetic energy gain due to the considerable magnetic moment of Rh atom (1.041 μ_B), which reduces total energy to a certain degree, hence a FM state is more stable than A-AFM and C-AFM states even though it is less stable compared to the ground G-AFM state.

In the Rh-termination, the 180° superexchange interaction disappears because of the absence of Fe layer above the Rh-terminated surface. The 90° superexchange interaction makes the A-AFM more stable than G-AFM. Instead, the magnetic energy gain of the surface Rh atom plays a key role in stabilizing FM. Hence, FM is the magnetic ground state in the Rh-terminated FeRh thin films. In the Fe-termination, on the other hand, G-AFM is most stable as in bulk since the 180° superexchange interaction still works.

In Fig. 3, calculated MCA energies, $E_{MCA} \equiv E(\rightarrow) - E(\uparrow)$, are presented as function of thickness for the Fe- and the Rh-terminated films in their for G-AFM and FM states. E_{MCA} 's for other magnetic states are also shown for comparison. From the definition of E_{MCA} , positive (negative) value implies perpendicular (parallel) magnetization to the surface normal. Interestingly, the Rh-termination in FM state shows quite strong persistent perpendicular MCA regardless of thickness, whereas the Fe-termination exhibits in-plane MCA for all magnetic states. In particular, $E_{MCA} = +2.1$ meV/□ of the Rh-termination is greater than 3d magnetic metals such as bulk Fe, Co, and Ni by two orders of magnitude and larger than magnetic films by several factors. From the fact that both the Fe-terminated FM states and the Rh-terminated G-AFM state show parallel MCA, the magnetic states are not a key factor in

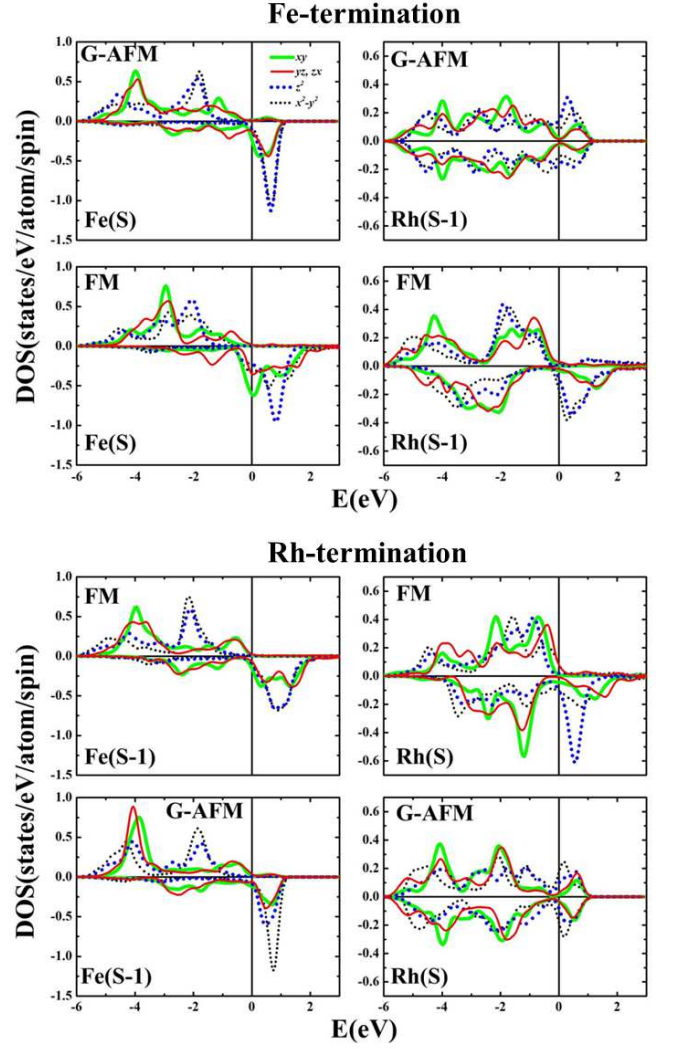


FIG. 4: Projected density of states of d orbitals of 9-ML FeRh film in the Fe-termination (upper panels) and the Rh-termination (lower panels) for FM and G-AFM states. S and S-1 indicate the top surface and subsurface layer, respectively.

determining MCA, but the surface termination is. Moreover, the saturated feature of $E_{MCA} = +2.1$ meV/□ with respect to the thickness implies that magnetism of the Rh surface plays a key role in determining the strong perpendicular MCA. To discuss the role of the thickness and the surface termination on magnetism as well as MCA, we present density of states (DOS) of the Fe- and the Rh-terminated 9-ML film is presented in Fig. 4, where left and right columns represent DOS's of Fe and Rh atoms for better comparison as in Fig. S2. First and second rows are for the Fe-terminated film in G-AFM and FM states; third and forth rows are for the Rh-terminated film in FM and G-AFM states. DOS features do not differ very much from the bulk, despite lifted degeneracies in e_g and t_{2g} states at the surfaces and some changes in surface atoms. In particular, DOS's of subsurface atoms are essentially the same as the bulk. This result confirms that the surface atoms indeed play

the key role in determining magnetism in film geometry, as saturated E_{MCA} with respect to thickness implies [see Fig. 3].

To confirm and analyze calculated results on MCA, additional calculations have been carried out using FLAPW method using GGA for 5-, 7-, and 9-ML Rh-terminated films. Results by FLAPW method are quite consistent with VASP method: i) FM is much more stable than G-AFM states, ii) magnetic moments of the surface Rh atoms are 1.107, 1.106, and 1.107 (Compare with SI Table S2) for 5-, 7-, and 9-ML, respectively, and iii) $E_{MCA} = +1.97$, $+2.41$, and 2.10 meV/□ (cf. Fig. 3), respectively. E_{MCA} 's are further decomposed into individual atomic contribution and different spin-channels[31]. It is found that the surface Rh atom with stronger spin-orbit coupling[32–34] and the $\uparrow\downarrow$ channel play a dominant role in determining MCA. Results using FLAPW adopting conventional von Barth-Hedin local spin density approximation (LSDA) are also listed in SI Table S3.

The role of the surface Rh layer in determining perpendicular MCA is well manifested in DOS: the lifted degeneracy of e_g states makes peak from d_{z^2} more prominent in the minority spin band, which is just above the Fermi level. This peaked d_{z^2} state contributes significantly to perpendicular MCA through $\langle yz/zx, \uparrow | L_X | z^2, \downarrow \rangle$ matrix[31] in the Rh-termination.

In order to elucidate the magnetic behavior when the FeRh(001) films are under an applied magnetic field or heat, we present total energy of the Fe-terminated FeRh(001) thin film as a function of angle between magnetic orientations of the closest Fe atoms.[See SI Fig. S3]. The energy barrier of the AFM-to-FM transition under an applied magnetic field is reduced with decreasing of thickness. This information might be useful in designing spintronics devices such as an AFM memory[8–10] and HAMR[5–7].

In summary, magnetism of the Fe- and the Rh-terminated FeRh (001) are studied for various film thicknesses. The origin of stability of G-AFM in bulk is well explained in the framework of Goodenough-Kanamori-Anderson rules on the super-exchange interaction, where subsidiary Zener-type direct exchange interaction and magnetization energy are also taken into account. The thickness and the surface termination turn out really significant as the two terminations give different magnetic ground state. The Fe-termination is stabilized in G-AFM as in bulk, while the energy difference between G-AFM and FM is greatly reduced. On the other hand, the Rh-termination strongly prefers FM when films are thinner than 15-ML. Furthermore, the Rh-termination in FM state exhibits quite strong perpendicular MCA, 2.10 meV/□, which is greater than bulk 3d convention magnetic metals by two orders of magnitude and larger than 3d magnetic films by several factors. Utilizing the thickness and the surface-termination dependent magnetism of FeRh film, highly desirable materials can be tailored as required by spintronics devices.

This work was supported by the Priority Research Centers Program (2009-0093818) and the Basic Science Research Program (2010-0008842) through the National Research Foundation funded by the Ministry of Education of Ko-

rea. ABS acknowledges support from the Czech Rep. grant (GACR 14-37427G).

* Email address: sonny@ulsan.ac.kr

† Email address: schong@ulsan.ac.kr

- [1] M. Manekar and S. B. Roy, J. Phys. D: Appl. Phys. **41**, 192004 (2008).
- [2] S. A. Nikitin, G. Myalikguliev, M. P. Annaorazov, A. L. Tyurin, R. W. Myndyevb, and S. A. Akopyan, Phys. Lett. A **171**, 234 (1992).
- [3] M. R. Ibarra and P. A. Algarabel, Phys. Rev. B **50**, 4196 (1994).
- [4] M. Sharma, H. M. Aarbogh, J.-U. Thiele, S. Maat, E. E. Fullerton, and C. Leighton, J. Appl. Phys. **109**, 083913 (2011).
- [5] S.O. Mairager *et al.* Phys. Rev. Lett. **108**, 087201 (2012).
- [6] N. T. Nam, W. Lu, and T. Suzuki, J. Appl. Phys. **105**, 07B515 (2009)
- [7] J.-U. Thiele, S. Maat, and E. E. Fullerton, Appl. Phys. Lett. **82**, 2859 (2003).
- [8] S. Loth, S. Baumann, C. P. Lutz, D. M. Eigler, and A. J. Heinrich, Science **335**, 196 (2012).
- [9] X. Martí, I. Fina, C. Frontera, J. Liu, P. Wadley, Q. He, R. J. Paull, J. D. Clarkson, J. Kudrnovsky, I. Turek, J. Kunes, D. Yi, J.-H. Chu, C. T. Nelson, L. You, E. Arenholz, S. Salahuddin, J. Fontcuberta, T. Jungwirth, and R. Ramesh, Nature Mater. **13**, 367 (2014).
- [10] C. Baldasseroni *et al.* Appl. Phys. Lett. **100**, 261401 (2012).
- [11] A. B. Shick, S. Khmelevskiy, O. K. Mryasov, J. Wunderlich, and T. Jungwirth, Phys. Rev. B **81**, 212409 (2010).
- [12] B. G. Park, J. Wunderlich, X. Martí, V. Holý, Y. Kurosaki, M. Yamada, and T. Jungwirth, Nature Mater. **10**, 347 (2011).
- [13] R. Duine, Nature Mater. **10**, 345 (2011).
- [14] X. Martí, B. G. Park, J. Wunderlich, H. Reichlov, Y. Kurosaki, M. Yamada, and T. Jungwirth, Phys. Rev. Lett. **108**, 017201 (2012).
- [15] Y. Y. Wang, C. Song, B. Cui, G. Y. Wang, F. Zeng, and F. Pan, Phys. Rev. Lett. **109**, 137201 (2012).
- [16] D. Petti, E. Albisetti, H. Reichlov, J. Gazquez, M. Varela, M. Molina-Ruiz, and R. Bertacco, Appl. Phys. Lett. **102**, 192404 (2013).
- [17] C. Baldasseroni, G. K. Palsson, C. Bordel, S. Valencia, A. A. Unal, F. Kronast, and F. Hellman, J. Appl. Phys. **115**, 043919 (2014).
- [18] R. O. Cherifi, V. Ivanovskaya, L. C. Phillips, A. Zobelli, I. C. Infante, S. Jacquet, V. Garcia, S. Fusil, P. R. Briddon, N. Guiblin, A. Mougin, A. A. Unal, F. Kronast, S. Valencia, B. Dkhil, A. Barthelémy, and M. Bibes, Nature Mater. **13**, 345 (2014).
- [19] C. Bordel, J. Juraszek, D. W. Cooke, C. Baldasseroni, S. Mankovsky, J. Minr, H. Ebert, S. Moyerman, E.E. Fullerton, and F. Hellman, Phys. Rev. Lett. **109**, 117201 (2012).
- [20] J. B. Goodenough, *Magnetism and the Chemical Bond* (Interscience Publisher, New York, 1963).
- [21] P. W. Anderson, Chapter 2, in *Magnetism*, edited by G. T. Rado and H. Shul (Academic Press, New York, 1963).
- [22] C. Zener, Phys. Rev. **81**, 440 (1951).
- [23] G. Kresse and J. Furthmüller, Phys. Rev. B **54**, 169 (1996).
- [24] E. Wimmer, H. Krakauer, M. Weinert, and A. J. Freeman, Phys. Rev. B **24**, 864 (1981) and references therein.
- [25] P. Blöchl, Phys. Rev. B **50**, 17953 (1994).
- [26] V. L. Moruzzi and P. M. Marcus, Phys. Rev. B. **46**, 2864 (1992).
- [27] G. Shirane, C. W. Chen, P. A. Flinn, and R. Nathans, J. Appl.

- Phys. **34**, 1044 (1964).
- [28] G. Shirane, C. W. Chen, and R. Nathans, Phys. Rev. **134**, A1547 (1964).
 - [29] W. Kim, S. C. Hong, J. Seo, S.-J. Oh, H. G. Min, and J.-S. Kim, Phys. Rev. B **70**, 174453 (2004).
 - [30] V. M. T. S. Barthem, A. Rogalev, F. Wilhelm, M. M. Sant'Anna, S. L. A. Mello, Y. Zhang, P. Bayle-Guillemaud, and D. Givord, Phys. Rev. Lett. **109**, 197204 (2012).
 - [31] D. S. Wang, R. Q. Wu, and A. J. Freeman, Phys. Rev. B **47**, 14932 (1993).
 - [32] D. Odkhuu, S. H. Rhim, N. Park, and S. C. Hong, Phys. Rev. B **88**, 184405 (2013).
 - [33] W. S. Yun, G. B. Cha, I. G Kim, S. H. Rhim, and S. C. Hong, J. Phys.: Cond. Matter **24**, 416003 (2012).
 - [34] S. C. Hong, W. S. Yun, and R. Q. Wu, Phys. Rev. B **79**, 054419 (2009).